Am J Physiol Lung Cell Mol Physiol 311: L538–L549, 2016.
First published July 15, 2016; doi:10.1152/ajplung.00139.2016.

CALL FOR PAPERS | *Biomarkers in Lung Diseases: from Pathogenesis to Prediction to New Therapies*

Role of mesothelin in carbon nanotube-induced carcinogenic transformation of human bronchial epithelial cells

Xiaoqing He,[1]* Emily Despeaux,[1]* Todd A. Stueckle,[1,2] Alexander Chi,[3] Vincent Castranova,[1] Cerasela Zoica Dinu,[4] Liying Wang,[2] and Yon Rojanasakul[1,3]

[1]*Department of Pharmaceutical Sciences, West Virginia University, Morgantown, West Virginia;* [2]*HELD, National Institute for Occupational Safety and Health, Morgantown, West Virginia;* [3]*WVU Cancer Institute, West Virginia University, Morgantown, West Virginia; and* [4]*Department of Chemical Engineering, West Virginia University, Morgantown, West Virginia*

Submitted 31 March 2016; accepted in final form 5 July 2016

He X, Despeaux E, Stueckle TA, Chi A, Castranova V, Dinu CZ, Wang L, Rojanasakul Y. Role of mesothelin in carbon nanotube-induced carcinogenic transformation of human bronchial epithelial cells. *Am J Physiol Lung Cell Mol Physiol* 311: L538–L549, 2016. First published July 15, 2016; doi:10.1152/ajplung.00139.2016.—Carbon nanotubes (CNTs) have been likened to asbestos in terms of morphology and toxicity. CNT exposure can lead to pulmonary fibrosis and promotion of tumorigenesis. However, the mechanisms underlying CNT-induced carcinogenesis are not well defined. Mesothelin (MSLN) is overexpressed in many human tumors, including mesotheliomas and pancreatic and ovarian carcinomas. In this study, the role of MSLN in the carcinogenic transformation of human bronchial epithelial cells chronically exposed to single-walled CNT (BSW) was investigated. MSLN overexpression was found in human lung tumors, lung cancer cell lines, and BSW cells. The functional role of MSLN in the BSW cells was then investigated by using stably transfected MSLN knockdown (BSW shMSLN) cells. MSLN knockdown resulted in significantly decreased invasion, migration, colonies on soft agar, and tumor sphere formation. In vivo, BSW shMSLN cells formed smaller primary tumors and less metastases. The mechanism by which MSLN contributes to these more aggressive behaviors was investigated by using ingenuity pathway analysis, which predicted that increased MSLN could induce cyclin E expression. We found that BSW shMSLN cells had decreased cyclin E, and their proliferation rate was reverted to nearly that of untransformed cells. Cell cycle analysis showed that the BSW shMSLN cells had an increased G2 population and a decreased S phase population, which is consistent with the decreased rate of proliferation. Together, our results indicate a novel role of MSLN in the malignant transformation of bronchial epithelial cells following CNT exposure, suggesting its utility as a potential biomarker and drug target for CNT-induced malignancies.

mesothelin; nanotubes; cancer; cell invasion; tumor formation

CARBON NANOTUBES (CNTS) HAVE unique physical and chemical properties that make them suitable for a variety of consumer and biomedical applications. Their electrical conductivity and strength are exploited with their integration into consumer products, including electronics and sports equipment. The ease of functionalization make CNTs ideal candidates for biosensors and drug delivery platforms (10, 32, 38). CNTs are fibrous in shape and resistant to chemical and high-temperature degradation. Therefore, CNTs exhibit asbestos-like properties (44). Because of the rapid growth of production, worker exposure to CNTs is increasingly likely, creating a potential human health hazard (10, 42).

Pulmonary toxicity following CNT exposure is of particular concern, as CNTs are small, low density, and easily aerosolized (32). As with other nanoparticles, the toxicity of CNTs depends heavily on the dose, exposure route, and particle physical properties (38, 42). Variations in these parameters often make it difficult to compare published outcomes. However, the consensus is that inhalation of CNTs are likely detrimental to human health, but the full scope and mechanisms of the damage are still unclear (11).

Much of what is known about CNT toxicity comes from acute, high-dose exposures, which result in transient inflammation and fibrosis (7, 42). In reality, chronic, low-dose exposures are more likely (42), meaning that chronic exposure models are needed to determine meaningful occupational exposure limits. Additionally, CNTs are not degraded in vivo and their persistent presence, even at very low doses, can cause oxidative stress (42) and DNA damage (7). Over time, this damage could contribute to the development of cancer. However, the molecular mechanisms underlying this transformation are currently unknown.

To better understand the mechanism of CNT-induced carcinogenesis, we previously generated an in vitro chronic CNT exposure model by culturing human bronchial epithelial (BEAS-2B) cells with single-wall carbon nanotubes (SWCNTs) (0.02 $\mu g/cm^2$) for 6 mo (21, 47). These chronic SWCNT-exposed (BSW) cells had greater malignant morphology and behavior than their passage-matched parental cells, including increased proliferation rates, increased resistance to apoptosis (30, 47), and increased tumor formation in vivo (21, 47).

The malignant phenotype noted after chronic exposure to subacute doses of SWCNTs results from the interaction of many factors, including changes in regulation of a variety of cell processes (apoptosis, invasion/attachment, cell cycle reg-

* X. He and E. Despeaux contributed equally to this work.

Address for reprint requests and other correspondence: Y. Rojanasakul, Dept. of Pharmaceutical Sciences, West Virginia Univ., Morgantown, PO Box 9530, Morgantown, WV 26506 (e-mail: yrojan@hsc.wvu.edu).

ulation, etc.). The mechanisms causing these changes have not been fully described, but, given the similarities between CNTs and asbestos, it is possible that the pathologies could develop through similar mechanisms.

Mesothelin (MSLN), a 40-kD cell-surface protein of unknown physiological significance, is found in very few normal tissues. The MSLN gene encodes a 70-kD precursor protein that is cleaved into the 40-kD cell-surface mature MSLN fragment and a 30-kD soluble fragment. Mature MSLN is detectable in nearly all mesotheliomas and ~30% of all cancers (29). Overexpression of MSLN in lung adenocarcinomas is correlated with decreases in both overall and relapse-free survival (16). Although neither the normal or pathological role of MSLN is explicitly known, it has been suggested that MSLN may promote the development of malignancy by affecting cell adherence (41), cell survival and proliferation (16, 19, 41), invasion and migration (16), apoptosis resistance, and chemosensitivity (41). The soluble MSLN fragment is detectable in the serum of many cancer patients, and its presence has been investigated as a potential biomarker for lung adenocarcinoma, mesothelioma (37), pancreatic cancer (19, 41), and ovarian cancer (12).

Since MSLN is thought to play a role in carcinogenesis, this study was designed to determine the functional role of MSLN in SWCNT-transformed bronchial epithelial cells (BSW). A stably transfected MSLN knockdown line (BSW shMSLN) was generated and used to evaluate the effects of MSLN knockdown on cell migration, invasion, colony formation, and tumor sphere formation in vitro, as well as tumorigenesis and metastasis in vivo. An MSLN-overexpressing BEAS-2B line, B2B/MSLN, was also generated to determine if MSLN overexpression alone could induce the same in vitro malignant phenotypic changes as those previously noted in the BSW cells. The mechanism by which MSLN could contribute to these behaviors was investigated by Ingenuity Pathway Analysis, which suggested that MSLN induced cyclin E, leading to cell cycle dysregulation. The effects of MSLN on cyclin E and cell cycle regulation were verified experimentally.

MATERIALS AND METHODS

Patient tumor samples. Human lung tissue lysates were purchased from Protein Biotechnologies (Ramona, CA). Samples from lung tumors and adjacent healthy tissue were provided as pairs. Six large cell carcinomas, two squamous carcinomas, and one adenocarcinoma were tested.

Cell culture. Nontumorigenic human bronchial epithelial BEAS-2B cells were cultured with SWCNT (0.02 μg/cm^2) for 6 mo to generate CNT-transformed bronchial epithelial cells (BSW), as previously described (21, 47). This cell model has been reported to be an appropriate model for in vitro lung carcinogenesis studies (28, 48). BSW cells were maintained in Dulbecco's modified Eagle medium (DMEM) supplemented with 5% fetal bovine serum (FBS), 2 mM l-glutamine, 100 units/ml penicillin and 100 μg/ml streptomycin (Gibco, Gaithersburg, MA). A549 cells, human lung carcinoma alveolar type II epithelial cells, were cultured in DMEM supplemented with 5% fetal bovine serum (FBS), 2 mM l-glutamine, 100 units/ml penicillin and 100 μg/ml streptomycin (Gibco). Nonsmall cell lung cancer H460 cells were cultured in RPMI 1640 medium supplemented with 5% FBS, 2 mM l-glutamine, and 100 units/ml penicillin/streptomycin. With the exception of laboratory-generated BSW and passage control BEAS-2B cells, all cells were purchased from ATCC (Manassas, VA). All cells were maintained in a humidified atmosphere of 5% CO_2 at 37°C.

Generation of stable MSLN knockdown BSW cells. Stable MSLN knockdown BSW cells and vector-transfected control cells were generated by using shMSLN lentiviral plasmid vector or scrambled shRNA vector (OriGene Technologies, Rockville, MD) and transfected by the Amaxa Nucleofector II electroporation method (Lonza, Walkersville, MD). Stable transfected single clones were selected with 5 μg/ml of puromycin. MSLN knockdown was verified by Western blotting.

Transient MSLN overexpression in B2B cells. MSLN overexpression was transiently induced in BEAS-2B cells with plasmid DNA (pEasy-MSLN-iCre-HA-Flag, plasmid No. 31305, Addgene, Cambridge, MA) and FuGENE HD transfection reagent (Promega, Madison, WI), according to the manufacturers protocol. At 24 h after the transfection, MSLN protein expression levels were assessed by Western blotting. MSLN-overexpressing BEAS-2B cells (B2B/MSLN) were used in migration, invasion, and colony formation assays.

Cell proliferation. MSLN knockdown and vector control cells were seeded at a density of 1.5×10^4 cells per well in 100 μl of media in a 96-well plate (Fisher Scientific, Waltham, MA). After 24, 48, or 72 h, 20 μl of CellTiter 96 Aqueous One Solution (Promega, Madison, WI) were added to each well, and the cells were incubated at 37°C for an additional 3 h. Viable cells cleave the reagent's tetrazolium salt to a soluble formazan dye, resulting in a color change proportional to the number of live cells. Absorbance was measured at 490 nm, with a reference wavelength at 630 nm, by using a BioTek Plate Reader (BioTek, Winooski, VT).

Soft agar colony formation assay. BSW shMSLN and BSW shC cells (2,500 cells) were suspended in 0.5 ml of culture medium and mixed with equal amount of 0.7% agar to a final agar concentration of 0.35%. The 1 ml cell/agar suspensions were immediately plated onto a 6-well plate coated with 0.5% agar in culture medium (1 ml/well). Colonies were examined under a light microscope after 2 wk of culture. Colonies were counted if >50 cells. To assess the self-renewing property of cells, colonies were collected by gentle centrifugation, dissociated into single-cell suspensions, filtered and cultured under conditions described above (second colony formation).

Tumor sphere formation assay. Tumor sphere assay was performed under stem cell selective (nonadherent and serum-free) conditions as previously described (49). Briefly, 5×10^3 cells were suspended in 0.8% methylcellulose (MC)-based serum-free medium (Stem Cell Technologies, Vancouver, Canada) supplemented with 20 ng/ml of epidermal growth factor (BD Biosciences, San Jose, CA), basic fibroblast growth factor and 4 mg/ml of insulin (Sigma, St. Louis, MO) in an ultra-low adherent 6-well plate. Cells were then cultured for 2 wk. Tumor spheres were examined under a light microscope. To assess the self-renewing property of cells, spheres were collected by gentle centrifugation, dissociated into single-cell suspensions, filtered, and cultured under conditions described above (second-sphere formation).

Cell migration and invasion assays. In vitro cell migration was determined with a 24-well Transwell unit with polycarbonate (PVDF) filters (8-μm-pore size). In vitro cell invasion was performed with a BD Matrigel invasion chamber (BD Biosciences). Briefly, cells at the density of 1.5×10^4 cells per well (migration) or 3×10^4 cells per well (invasion) were seeded into the upper chamber of the Transwell unit in serum-free medium. The lower chamber of the unit was filled with a normal growth medium containing 5% FBS. Chambers were incubated at 37°C in a 5% CO_2 atmosphere for 48 h. The nonmigrating or noninvading cells were removed from the inside of the insert with a cotton swab. Cells that migrated or invaded to the underside of the membrane were fixed and stained with Diff-Quik (Dade Behring, Newark, DE). Inserts were visualized and scored under a light microscope (Leica DM IL). Number of migrating and invading cells were counted. Results represent the means ± SD from 10 fields evaluated.

Immunoblotting. Cells were washed twice with ice-cold PBS and lysed on ice with modified RIPA buffer containing protease and phosphatase inhibitor mixture (Roche Molecular Biochemicals, Indianapolis, IN) for 30 min. The lysate was sonicated briefly and centrifuged at 14,000 *g* for 20 min. Cell lysates (40 μg of protein) were fractionated by 10% sodium dodecyl sulfate-polyacrylamide gel electrophoresis (SDS-PAGE) and transferred onto polyvinylidene difluoride membranes (PVDF) (Bio-Rad Laboratories, Hercules, CA). The transferred membranes were blocked for 1 h with 5% nonfat dry milk in TBST (25 mM Tris-HCl, pH 7.4, 125 mM NaCl, 0.05% Tween 20) followed by MSLN (ab96869, Abcam, Cambridge, MA) or cyclin E (Cell Signaling, Danvers, MA) primary antibody at 4°C overnight with gentle shaking. Membranes were washed three times with TBST for 10 min each, followed by incubation with a horseradish peroxidase-conjugated β-actin secondary antibody (A5441, Sigma) for 1 h at room temperature. Protein bands were visualized with enhanced chemiluminescence detection reagents from Millipore (Billerica, MA). Actin was blotted to ensure equal loading of the samples, and data were quantified with image J densitometry software.

Flow cytometry. MSLN knockdown and scrambled shRNA control cells were seeded overnight in 6-well plates (Fisher Scientific) at a concentration of 3×10^5 cells/well. The cells were trypsinized, collected, washed twice with PBS, and fixed overnight in 70% ethanol (Fisher Scientific) at −20°C. Subsequently, the cells were washed and suspended in 0.2% Tween 20 (Sigma) PBS solution for 15 min at 37°C, followed by RNase A (180 μg/ml) for 15 min at room time temperature. The cells were then stained with propidium iodide PBS (50 μg/ml; Sigma) for 15 min at room temperature. Changes in DNA content were determined with a BD LSR Fortessa Flow cell analyzer (BD Biosciences) and BD FACS Express 5 software. The forward scatter and side scatter were used to gate the majority of the cell population; 20,000 events were collected for each sample. The selection of the cells was based on knowing that in the G0/G1 phase (before DNA synthesis) cells have a defined amount of DNA (i.e., a diploid chromosomal DNA content) and double that amount in the G2 or M phase (G2/M, i.e., a tetraploid chromosomal DNA content). During the S phase (DNA synthesis), cells contain between one to two DNA levels.

Tumor xenograft mouse models. Animal care and experimental procedures described in this study were performed in accordance with the Guidelines for Animal Experiments at West Virginia University with the approval of the Institutional Animal Care and Use Committee (IACUC No. 15-0702). Immunodeficient NOD/SCID-γ mice, strain NOD Cg-Prkdcscid Il2rgtm1Wjl/SzJ (NSG; Jackson Laboratory, Bar Harbor, ME) were maintained under pathogen-free conditions within the institutional animal facility. Food and tap water were given ad libitum. Mice (6 per group) were subcutaneously injected with 5×10^5 cells of BSW with shMSLN or shControl stable knockdown cells suspended in 100 μl of ExtraCel hydrogel (Advanced BioMatrix, San Diego, CA). Mice were inspected daily for any signs of distress such as weight loss, hunching, failure to groom, or red discharge from the eyes. After 30 days, mice were euthanized and tumors were dissected and weighted. Metastatic nodules were counted from the surface on the intestine, liver, and lungs. Liver and lung tumor specimens were dissected into 5-μm sections and stained with hematoxylin and eosin to confirm cancer histology and metastasis in organs. All tissue sectioning and staining were performed at the West Virginia University Pathology Laboratory for Translational Medicine.

Immunostaining. Lung and liver sections in paraffin were deparaffinized and rehydrated. Antigens were retrieved with 10 mM of sodium citrate solution in the microwave for 20 min. The slides were then blocked with 3% BSA/0.1% Tween in 1X PBS blocking buffer for 1 h and were incubated with antihuman MSLN antibody (Abcam) at a dilution of 1:500 or antihuman mitochondria antibody (EMD Millipore, Temecula, CA) at a dilution of 1:100 overnight at 4°C. After washing with PBS three times, the slides were incubated with biotinylated secondary antibodies for 1 h, followed by avidin-biotin complex reagent (Vector Laboratories, Burlingame, CA), and detected with DAB kit (Vector Laboratories). After color development, the slides were counterstained with hematoxylin, dehydrated, and mounted with Permount mounting medium (Fisher Scientific). Images were taken with a light microscope with the SimplePCI 6 software (Compix, Cranberry, PA).

Ingenuity pathway analysis. To further understand MSLN's role in promoting the observed cancer cell phenotype, we examined the potential signaling pathways within BSW cells. Whole genome mRNA microarray data from our previous work (NCBI GEO Accession No. GSE56104) was uploaded into Ingenuity Pathway Analysis (Qiagen). All known mRNA and miRNA signaling associations with MSLN were plotted along with differential gene expression of BSW vs. passage control BEAS-2B cells (30). Genes and miRNA were excluded from the network if the relationship with MSLN was not reported in lung tissue. Because of the complexity of the network and aggressive, metastatic ability of BSW cells, genes only known to play a role in metastatic and stage IV lung cancer were kept in the MSLN network. Lastly, predictive activation/inhibition analysis of both upstream and downstream genes from MSLN was conducted by using *Z* scores. Based on the observed significant MSLN protein overexpression, we evaluated upstream and downstream targets with a predicted MSLN activation. These predictions were overlaid on the MSLN signaling network if $Z \pm 2$.

Statistics. Results were expressed as means ± SD. All values were derived from at least three independent experiments. Differences between groups were assessed by analysis of variance (ANOVA) followed by Student's *t*-test. For all analysis, two-sided *P* values of ≤0.05 were considered statistically significant.

RESULTS

Mesothelin expression is increased in human lung tumors and lung cancer cell lines. As reports on the pervasiveness of MSLN in human cancers vary widely, we first verified that MSLN was detectable in human lung tumors lysates. MSLN expression was assessed in 10 human lung tumor samples and corresponding adjacent, healthy tissue controls (Fig. 1*A*). Samples included six large cell carcinomas, three squamous cell carcinomas, and one adenocarcinoma. None of the control samples had notable MSLN expression. However, 5 of the 10 tumor samples had increased MSLN expression, ranging from 2- to 10-fold more MSLN than the corresponding normal controls (Fig. 1*B*).

To validate the differential expression of MSLN in malignant vs. nonmalignant cell lines, MSLN expression was assessed in noncancerous BEAS-2B cells, two lung cancer lines (A549, H460), and BSW cells, the previously generated SWCNT-transformed human bronchial epithelial line (47) (Fig. 1*C*). BEAS-2B cells had a lower level of MSLN expression than both the BSW cells and the lung cancer lines, A549 (adenocarcinoma) and H460 (large cell carcinoma) (Fig. 1*D*). Even though the BSW cells originated from the noncancerous BEAS-2B cells, their MSLN expression was on par with the cancer cell lines.

MSLN knockdown BSW cells are less aggressive than BSW cells in vitro and in vivo. To determine the functional role of MSLN in the expression of a more malignant phenotype by BSW cells, BSW cells were stably transfected with either MSLN short-hairpin (sh)RNA (shMSLN) or a vector control (shC). Western blot analysis (Fig. 2, *A* and *B*) showed that MSLN was decreased substantially in the shMSLN-transfected cells (BSW shMSLN). MSLN was decreased to nearly unde-

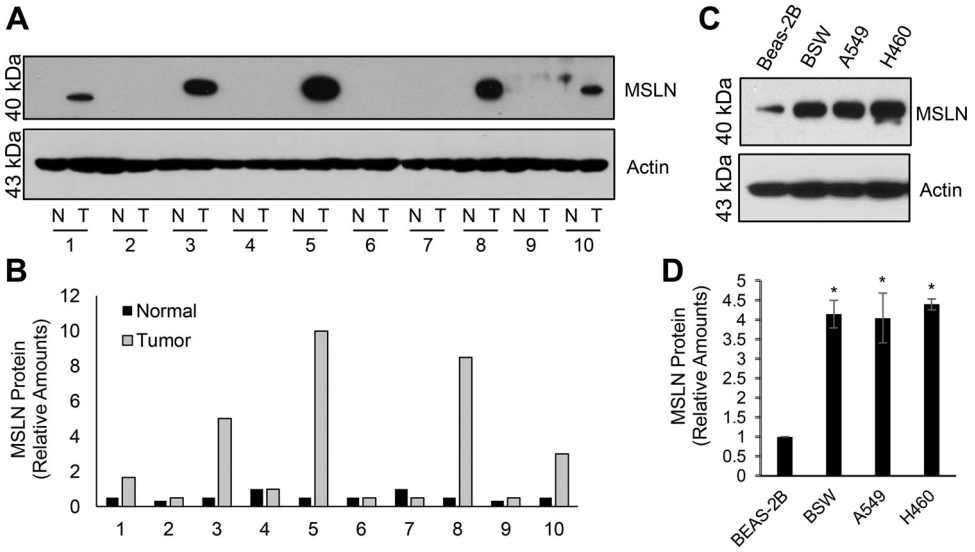

Fig. 1. MSLN is overexpressed in lung cancer. *A*: Western blot for MSLN in pairs of lung tumor lysates (T) and normal tissue controls (N) from the same patients. *Pairs 1–6* are large cell carcinomas, *pairs 7–9* are squamous cell carcinomas, and *pair 10* is adenocarcinoma. *B*: quantification of tumor MSLN expression, relative to actin. *C* and *D*: Western blot and quantification of MSLN in noncancerous bronchial epithelial cells (BEAS-2B), CNT-transformed BSW cells, and in two established lung cancer cell lines (A549 and H460). $*P < 0.05$ vs. BEAS-2B.

tectable levels in two clones (BSW shMSLN-1 and BSW shMSLN-5), and these clones were selected for further study.

Colony formation on soft agar is used to assess anchorage-independent cell growth in vitro, a hallmark of malignant transformation (5). MSLN knockdown cells (BSW shMSLN) formed significantly fewer colonies on soft agar than BSW controls (BSW shC) (23.7 ± 5.1 vs. 53.0 ± 9.9) and the colonies that did form were smaller than those formed by the BSW controls (Fig. 2, *C* and *E*). Although noncancerous cells are not usually expected to form colonies on soft agar, it has been noted that BEAS-2B cells form small, slow-growing colonies despite their nonmalignant origins (40, 45). Previously, it was shown that BSW cells formed eight times more colonies than passage-matched BEAS-2B cells (47).

Tumor spheres form from the proliferation of cancer stem cells and the number of tumor spheres that form is indicative of the relative amount of cancer stem cells in the culture (2). BSW shMSLN cells formed significantly fewer tumor spheres than BSW shC (50.2 ± 10.9 vs. 81.0 ± 9.7), and the spheres formed by the BSW shMSLN cells were overall smaller than those formed by BSW shC (Fig. 2, *D* and *F*).

To determine if the reduction in colony formation was due specifically to the decrease in MSLN, the experiments were repeated with a MSLN-overexpressing line. BEAS-2B cells were transiently transfected to overexpress MSLN (B2B/MSLN) (Fig. 2*G*). After MSLN overexpression was verified, B2B/MSLN colony formation on soft agar was assessed. B2B/MSLN formed substantially more colonies than B2B cells (6.5 ± 2.17 vs. 0.17 ± 0.51), and the colonies that formed were overall much larger than those seen with B2B cells (Fig. 2, *H* and *I*). Next, the effects of MSLN on cell migration and invasion were assessed. Migration was quantified by a Transwell system with 8-μm pores in the barrier. Cells that crossed the pores in the barrier were stained and counted (Fig. 3, *A* and *C*). The BSW vector control cells (BSW shC) had 2.6 times as many migrated cells as the MSLN knockdown cells (BSW shMSLN). Previously, BSW cells were shown to migrate twice as much as passage-matched BEAS-2B controls (47).

Invasion was quantified in a similar manner to migration, except a thin layer of extracellular matrix was added to form a barrier over the pores in the Transwell insert. In order for cells to cross through the barrier, they must first break down the extracellular matrix (18). BSW shMSLN demonstrated significantly (2.8 times) less invasion than BSW shC (Fig. 3, *B* and *D*). Previously, BSW cells were shown to invade three times as much as passage-matched BEAS-2B controls. Overall, the invasion and migration assays show that the reduction in MSLN significantly reduces the invasion and migration abilities of the BSW cells.

Next, the effect of MSLN overexpression on migration and invasion was assessed using B2B/MSLN cells. B2B/MSLN cells demonstrated significantly increased migration and invasion relative to B2B controls. Migration was increased sixfold (Fig. 3, *E* and *G*) relative to B2B controls, while invasion was increased fourfold (Fig. 3, *F* and *H*).

Since decreasing MSLN reduced the aggressiveness of BSW cells in vitro, we next assessed whether this translated to less severe in vivo behavior. While noncancerous cells, including the parental BEAS-2B line, are not expected to form tumors in nude mice (30), the transformed BSW cells have been shown to form injection site tumors in vivo (47). In our study, both BSW shMSLN and BSW shC cells formed injection site tumors in mice after 30 days, with the BSW shC cells forming tumors three times larger than those resulting from BSW shMSLN cells (Fig. 4, *A* and *B*).

We also assessed the ability of BSW tumors to metastasize by measuring surface tumor nodules in the abdominal and thoracic cavities. BSW shMSLN cells formed 15 times fewer metastatic nodules (average of 1 per mouse) than BSW shC cells (Fig. 4*C*). Mice injected with BSW shC had significantly greater tumor surface area in pulmonary and hepatic cross sections (56 ± 31.27 vs. 2.25 ± 4.5 cm^2) (Fig. 4*D*). Examination of hematoxylin and eosin stained liver and lung slices confirmed these findings, with tumor nodules present in the liver and lungs of mice treated with BSW shC cells, but not in mice treated with BSW shMSLN cells (Fig. 4*E*). Tissue sections were stained with antihuman mitochondrial and antihuman MSLN antibodies to ensure that the tumors had originated from the injected human cells (Fig. 4, *F* and *G*). Tissue staining

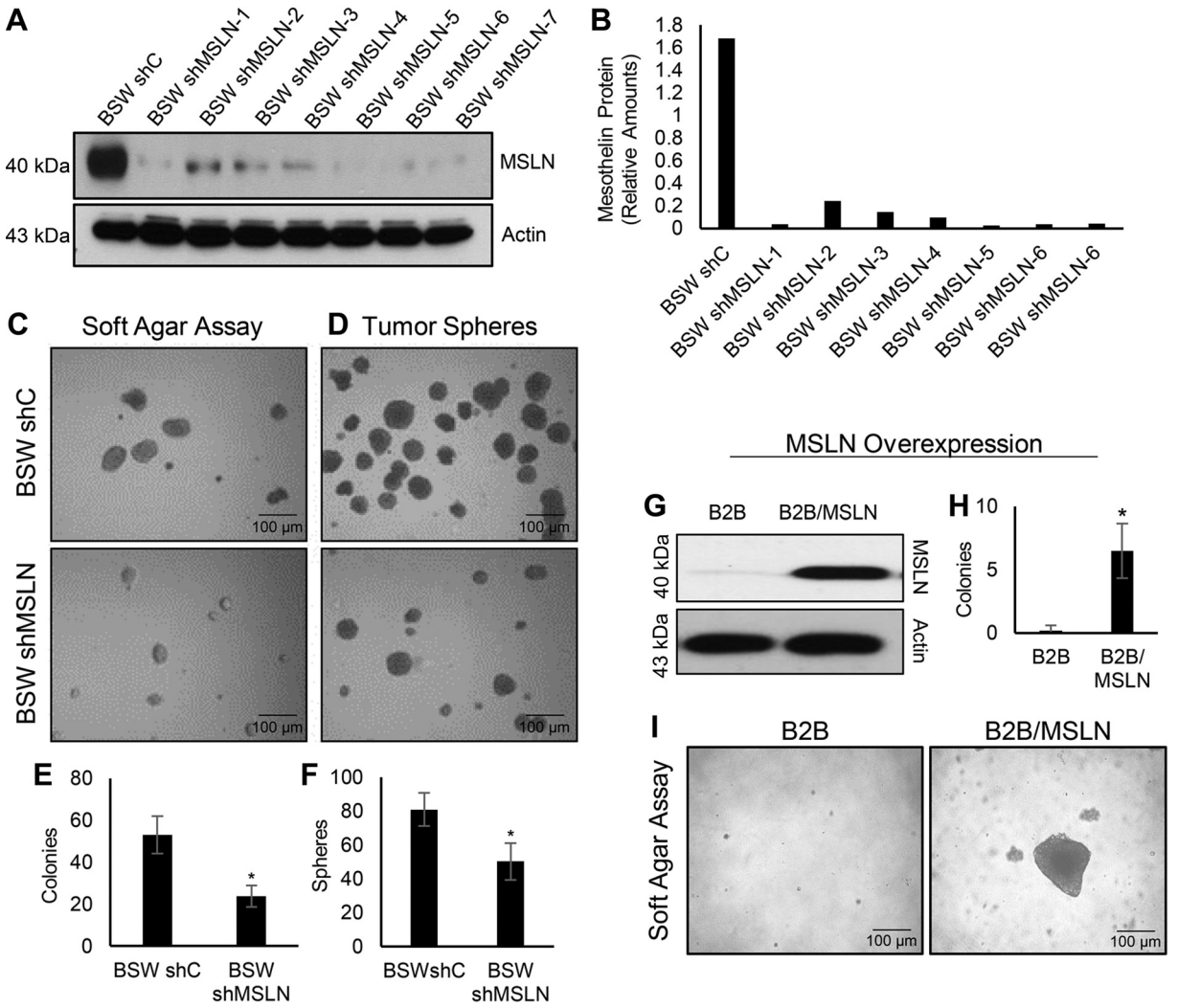

Fig. 2. Knockdown MSLN reduces soft agar colony and tumor sphere formation. *A* and *B*: Western blot and quantification of MSLN in several stable knockdown clones. *C*: representative images showing colony formation on soft agar of BSW shC and BSW shMSLN cells. *D*: representative images of tumor sphere formation of BSW shC and BSW shMSLN cells. *E*: quantification of colonies formed by BSW shC and BSW shMSLN cells. *F*: quantification of tumor spheres formed by BSW shC and BSW shMSLN cells. $*P < 0.05$ vs. BSW shC. *G*: Western blot of MSLN expression in B2B and B2B/MSLN cells. *H* and *I*: quantification and representative images of colonies formed by B2B and B2B/MSLN cells. $*P < 0.05$ vs. B2B.

results indicate that liver and lung metastatic lesions were of human origin and high in MSLN expression.

Mesothelin increases cyclin E, which drives more rapid cell proliferation. Possible mechanisms behind MSLN-driven malignancies were investigated by using Ingenuity Pathway Analysis (IPA) to determine the overlap between gene expression changes in BSW cells, as previously determined by whole genome mRNA microarray (23), and known relationships with overexpressed MSLN (Fig. 5). The prediction suggests that activated TNF, and K-ras ($z = 2.03$), mediators commonly increased with lung cancer, coupled with decreased and inhibited cyclin A, cyclin B and cyclin-dependent kinase 1 (CDK1) expression contribute to the induction of MSLN. Once MSLN has increased, it may increase the expression of matrix metalloproteinase (MMP) 7 and MMP-9, contributing to increased invasion, as well as stimulating increases in IL-6, Stat3, and cyclin E, which contribute to cell cycle dysfunction. MSLN is predicted to have an inhibitory effect on both p53 and the proapoptotic mediator BAX. Inhibition of p53 would complement the dysfunctional cell cycle progression resulting from the increase in cyclin E. Suppression of the antiapoptotic mediator BAX may shift the cells toward a more apoptosis-resistant state.

From the IPA data, it appears that MSLN induces cyclin E, which regulates cell cycle progression by acting as a gatekeeper at the G1/S phase transition. The IPA prediction was verified by Western blotting, which confirmed that cyclin E was highly expressed in BSW shC cells but barely detectable in either BSW shMSLN clone (Fig. 6, *A* and *B*), indicating that MSLN is an upstream regulator of cyclin E in these cells.

Increases in cyclin E, and the subsequent decreases in time spent in G1, can result in more rapid cell cycle progression and ultimately increased proliferation rates. The change in proliferation rate can be used to determine the functional significance of the changes in cyclin E and cell cycle distribution. A colorimetric proliferation assay, which allows for the determination of the number of metabolically active cells based on their conversion of the reagents tetrazolium salt to a water-

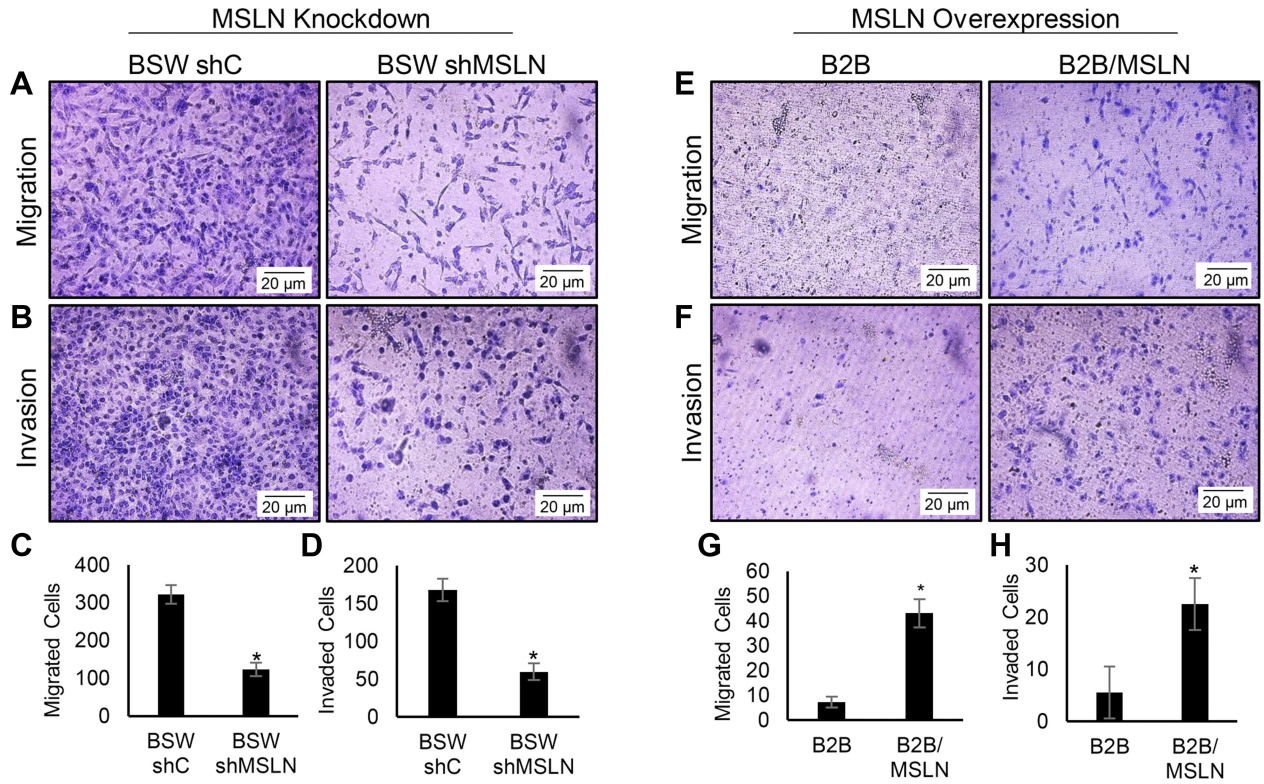

Fig. 3. MSLN expression increases migration and invasion in vitro. *A* and *B*: representative images of BSW shC and BSW shMSLN migration and invasion, stained with Diff-Quik. *C*: quantification of migrating BSW shC and BSW shMSLN cells. *D*: quantification of invading BSW shC and BSW shMSLN cells. $*P < 0.05$ vs. BSW shC. *E* and *F*: representative images of B2B and B2B/MSLN migration and invasion, stained with Diff-Quik. *G*: quantification of migrating B2B and B2B/MSLN cells. *H*: quantification of invading B2B and B2B/MSLN cells. $*P < 0.05$ vs. B2B.

soluble formazan dye, was used to quantify cell proliferation (Fig. 6*C*). By *day 3*, BSW shMSLN cells proliferated at half the rate of the BSW shC cells. In addition, BSW cells proliferate two to three times faster than passage-matched BEAS-2B controls (47). Thus knocking down MSLN nearly reverts cells to their original growth rate.

Flow cytometry was carried out to determine if the change in cyclin E levels correlated with a change in cell cycle distribution. Compared with the BSW shC cells, the BSW shMSLN cells had a greater percentage of the population in G2 phase and fewer cells progress to S phase (Fig. 7). Since cyclin E regulates the G1/S phase transition, the increased S population in the BSW shC cells serves as supporting evidence that the increase in cyclin E translates to a change in behavior. In addition, the decrease in the G2 population also indicates more rapid cell cycle progression.

DISCUSSION

Cancer develops from continuous dysregulation of the mechanisms controlling critical cell behaviors. Chemical and physical stimuli can contribute to both the initial cellular damage and the propagation of those effects. Assessing the potential carcinogenicity and carcinogenic mechanisms of new materials is often challenging due to the long latent periods between exposure and disease onset and the intricate molecular pathways regulating cell behavior (22). Rapid assessment of toxicity, as is possible with acute exposure models, does not always capture the full range of toxicological implications, particularly when used to assess biopersistent materials like asbestos and CNTs (42, 48).

CNTs have been likened to asbestos in terms of their fibrous structure and durability. As their integration into consumer products grows, understanding their toxicity has become a pressing public health matter (10, 42, 44). Their small, light, easily aerosolized structure makes inhalation exposures, and thus eventual lung toxicity, a primary concern (32). Once inhaled, SWCNTs can deposit in the deepest regions of the lung, the bronchoalveolar junctions and the alveoli themselves, where they persist for up to several months (22, 48). After an initial inflammatory response and the generation of reactive oxygen species (ROS), SWCNT persistence in the lung leads to the formation of granulomas and interstitial fibrosis (7, 35, 42, 48). Prolonged pulmonary inflammation and fibrosis increase the risk of developing lung cancer (22, 34). Additionally, SWCNTs may further increase the risk by damaging DNA and interfering with cell replication (7, 22, 34). Reported SWCNT genotoxicity, in in vitro and in vivo models, includes aneuploidy, centrosome fragmentation, damage to mitotic spindles, and increased numbers of micronuclei (22, 34, 36). Moreover, long-term exposure to CNTs induced malignant transformation of bronchial and small-airway epithelial cells (47, 48). SWCNT exposure in a mouse inhalation model also resulted in K-ras oncogene mutations, which have been implicated in carcinogenesis (34, 35). Despite the evidence for SWCNT-induced DNA damage, their status as an oncogenic initiator is still unconfirmed (48). However, a murine inhala-

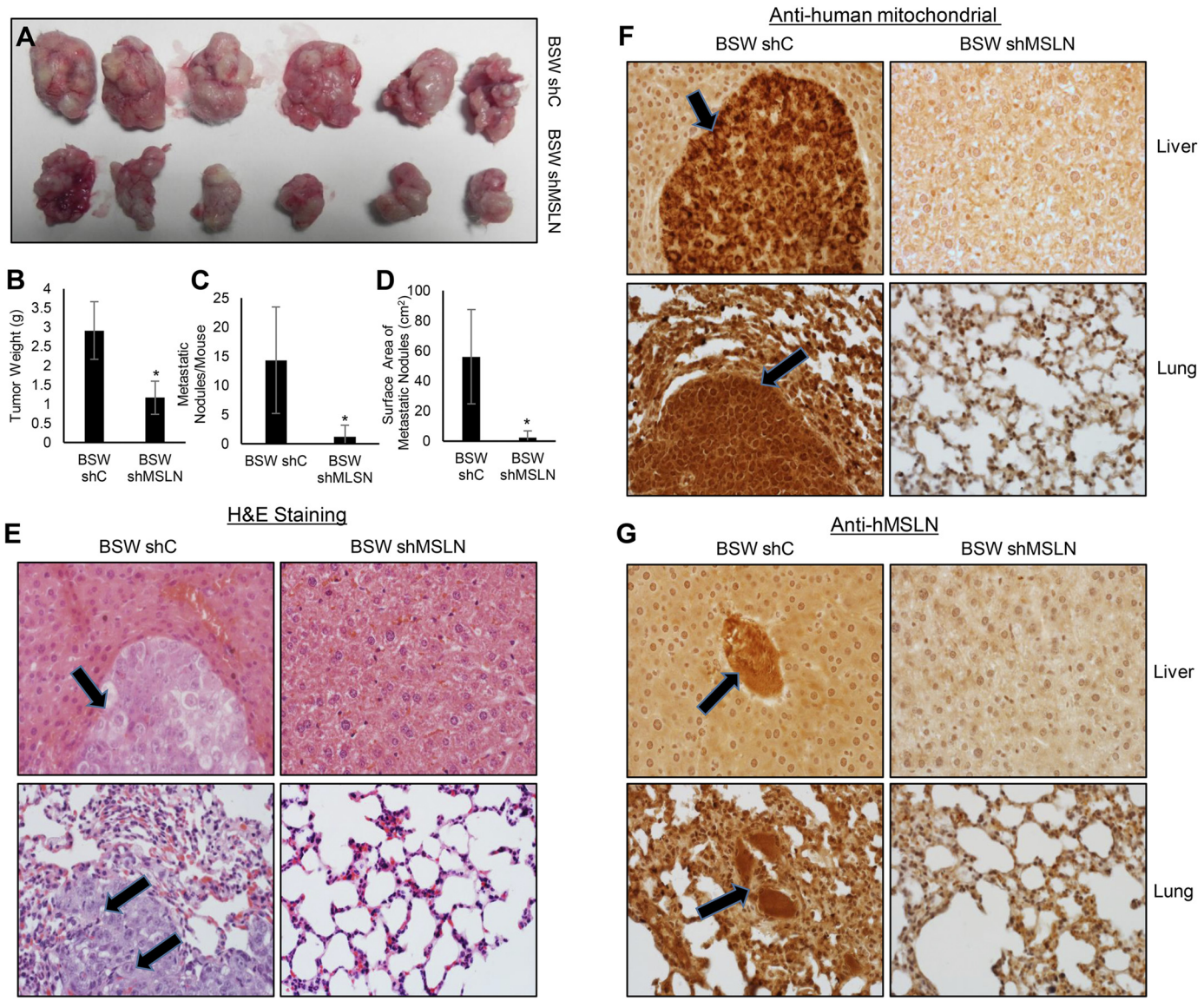

Fig. 4. MSLN regulates tumor growth and metastasis in vivo. *A*: injection site tumors. *B*: graphic representation of injection site tumor weights. C: number of thoracic and abdominal surface metastatic nodules. *D*: surface area of hepatic and pulmonary metastases. *E*: representative pulmonary and hepatic tissues with hematoxylin and eosin (H&E) staining. Arrows denote metastatic tumor nodules. *F* and *G*: immunostaining of human mitochondria and human MSLN in representative liver and lung sections of mice injected with BSW shC or BSW shMSLN. Arrows denote metastatic tumor nodules. $*P < 0.05$ vs. BSW shC.

tion study, using an initiator/promotor model, demonstrated that MWCNTs, specifically Mitsui-7 MWCNT, do act as tumor promotors (32).

To better understand the molecular mechanisms contributing to CNT carcinogenicity, we investigated the role of MSLN in the malignant transformation of lung epithelial cells chronically exposed to SWCNT. MSLN was historically associated with mesothelioma (37), which is primarily an asbestos-induced malignancy (48). MSLN has since identified in nearly 30% of all cancers, including a large number of lung (16), pancreatic (19, 41), and ovarian carcinomas (12).

The role of MSLN in lung cancer is not well defined, at least in part because its expression is highly variable even among patients with the same type and grade of tumor. For lung adenocarcinomas, MSLN has been detected in 39–83% of tumors (13, 16, 25–27), and tumor MSLN expression may be an independent predictor of relapse-free and overall survival (16). Increased MSLN expression is thought to be involved in cell adherence and chemotherapy resistance, as well as increased invasion and migration, cell proliferation, and anchorage-independent growth (41). However, as neither the physiologic role of MSLN nor its pathological mechanism is known, the varied prevalence of MSLN in tumors has made it difficult to discern whether or not MSLN has a functional role in the development of cancer.

Our BSW line, generated by exposing BEAS-2B cells to low doses of SWCNTs for 6 mo (47), offers a model to study the molecular and behavioral changes associated with malignant transformation of lung epithelial cells. This exposure model has been used to study the effects of chronic heavy metal exposures (28, 39) as well as chronic exposures to single (20, 21, 47, 48) and multiwall CNTs (44, 48). In addition, this

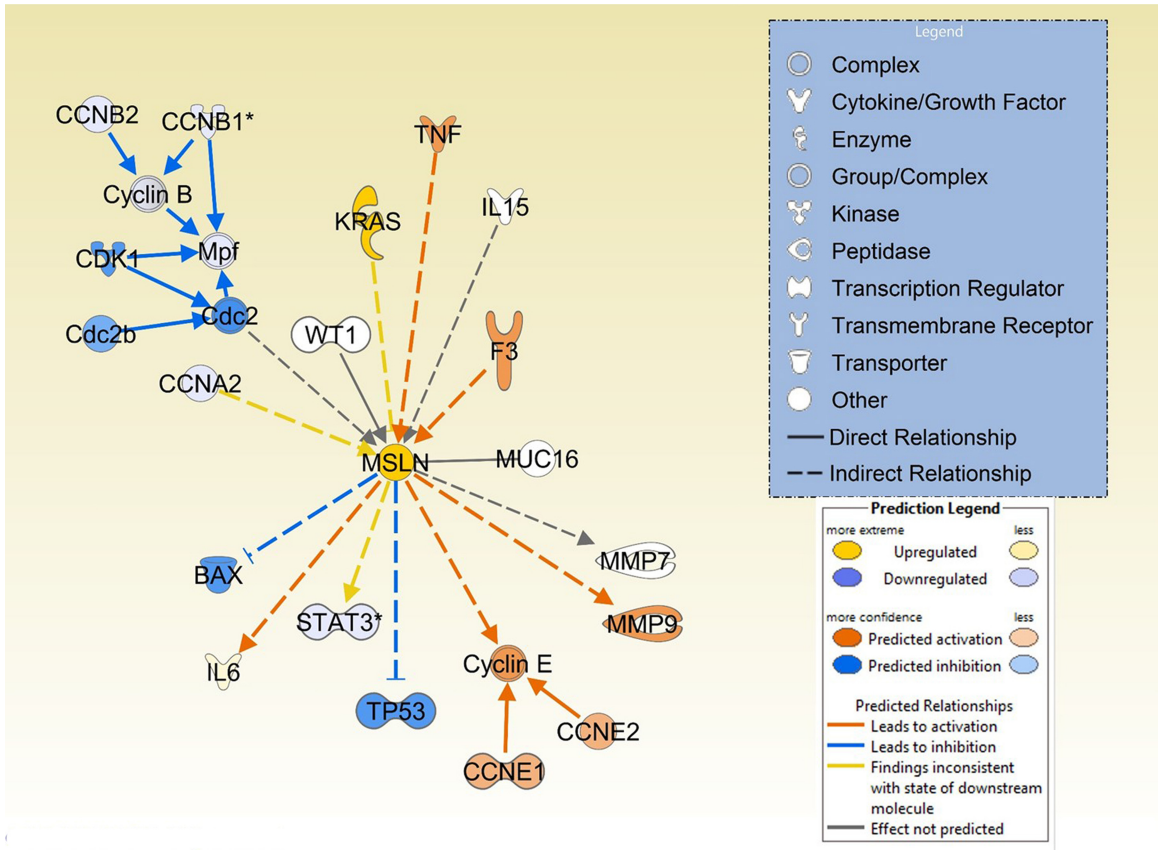

Fig. 5. Changes in gene expression when MSLN is increased in BSW cells. Ingenuity pathway analysis (IPA) was used to predict differentially expressed genes. Yellow to orange colors represent upregulation, and blue represent downregulation, compared with BEAS-2B passage-matched controls. Color intensity signifies fold change.

model was used to discern the differences in the toxicological effects of chronic in vitro exposure of lung epithelial cells to SWCNTs, MWCNTs, and asbestos, all of which are known to accumulate and trigger inflammation and fibrosis in vivo, vs. ultrafine carbon black, which exhibits lower in vivo toxicity and is not highly fibrogenic (48). Chronic in vitro exposure to nontoxic levels of SWCNTs, MWCNTs, and asbestos triggered neoplastic transformation, while cells exposed to ultrafine carbon black maintained a nonneoplastic phenotype with reduced cell proliferation, fewer colonies on soft agar, and an increase in genome-wide cell death signaling.

In the case of BSW cells, abnormal cell morphology was noted within the first 4 wk of exposure, and abnormal cell behavior was characterized after 6 mo of exposure (47). Although the mechanisms behind some aspects of this transformation, including the acquired apoptosis resistance (30, 47) and stemlike characteristics (21, 23), have been investigated, they do not account for all of the changes seen in the BSW cells, suggesting that there are likely additional, currently unidentified, contributing mechanisms. In this study, we found that BSW cells have greater MSLN expression than the parental BEAS-2B cells, and this model provided a unique platform to study the role of MSLN in malignant transformation and subsequent aggressive behavior.

BSW cells are morphologically and behaviorally distinct from the parental BEAS-2B line. These changes trend toward an overall more aggressive phenotype, including increased cell proliferation, invasion, migration, colony formation on soft agar, acquired resistance to apoptosis, induction of angiogenesis, and the ability to form tumors in vivo (47). These changes are consistent with those seen in other in vitro chronic CNT exposures (20, 44, 48). Interestingly, many of the changes seen in BSW cells correspond with previously suggested roles of MSLN.

In the present study, MSLN appears to contribute significantly to the increased metastatic potential of BSW cells. Metastases are responsible for the overwhelming majority of cancer deaths, because they are difficult to prevent or treat. After MSLN knockdown, invasion and migration were reduced significantly. Conversely, migration and invasion were increased when MSLN overexpression was induced in BEAS-2B cells. Lung cancer cells transduced to overexpress MSLN have previously been shown to have a 2-fold increase in both migration and invasion (16), which is similar to the 2.6- and 2.8-fold increase we noted in the BSW shC cells relative to the BSW shMSLN cells. MSLN-related increases in invasion and migration have also been reported in pancreatic cancer (16), ovarian cancer (6), and mesothelioma (24) cell lines.

Anchorage-independent growth, an in vitro hallmark of carcinogenic transformation, was also affected by changes in MSLN expression. We found that knocking down MSLN decreased soft agar colony and tumor sphere formation, whereas MSLN overexpression increased soft agar colony formation. This is in line with previous reports that MSLN-

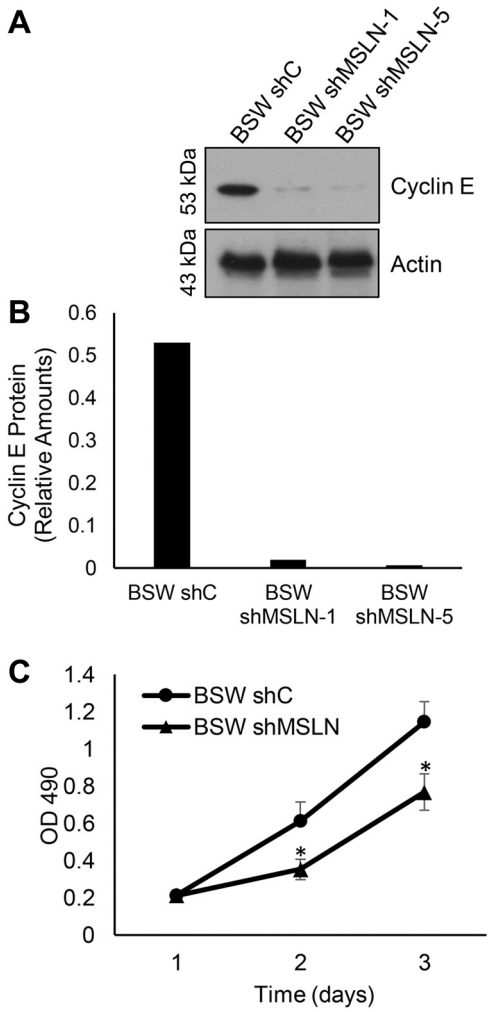

Fig. 6. MSLN regulates cyclin E and cell proliferation. *A* and *B*: Western blot and quantification of cyclin E in BSW shC and two MSLN knockdown clones. *C*: proliferation of BSW shC and BSW shMSLN cells, determined by using Promega Aqueous One-Step viability assay, which measures mitochondrial metabolic rate at 24 and 48 h after seeding. $*P < 0.05$ vs. BSW shC.

expressing breast cancer cells formed 1.5 times more colonies, and the colonies were twice the size, compared with non-MSLN-expressing controls (43). Similarly, silencing MSLN in mesothelioma cells results in reductions in both the number and size of colonies that form on soft agar (24).

A reduction in the aggressiveness of malignant cells in vitro should correlate with reduced tumor formation, both local and metastatic, in vivo. Our results show that knockdown of MSLN in our BSW cells did translate to significantly less metastases and reduced (but not eliminated) primary tumors in vivo. Immunohistochemistry indicated that metastatic lesions in BSW shC-treated mice were of human origin and expressed human MSLN. A previous study using pancreatic cancer cells that stably overexpressed MSLN showed that the MSLN-overexpressing cells resulted in larger tumors than the parental line (3). In rats with tuberous sclerosis, knocking out MSLN reduced the formation of kidney tumors, a change that was partially attributed to the MSLN knockdown cells being less able to bind to collagen (50).

Although elucidation of the specific mechanism for the decrease in metastases is beyond the scope of this study, it is likely that MSLN mediates cell-cell adhesion, and its overexpression aids the circulating tumor cells in attaching to new locations. This has been previously described in the context of ovarian cancer metastases attaching to the peritoneal lining via interactions between MSLN and the ovarian cancer antigen CA-125 (31). Additionally, in a kidney tumor model, MSLN knockout cells were less adherent to collagen (50). How this translates to other forms of cancer is not yet known, but further studies of this interaction in other lines, including BSWs, have the potential to enhance our understanding of the metastatic process.

The mechanism by which MSLN mediates metastasis may be related to its normal function. MSLN is typically found on the apical surface of mesothelial linings (27, 31) and is often (but not exclusively) seen on the apical surface or leading edge of tumors (1, 8, 9, 33). This is similar to the localization and effects of CA-125, the ovarian cancer antigen, and may explain why the coexpression of MSLN and CA-125 results in worse outcomes than either alone (31). This might also point toward MSLN having a similar function to CA-125.

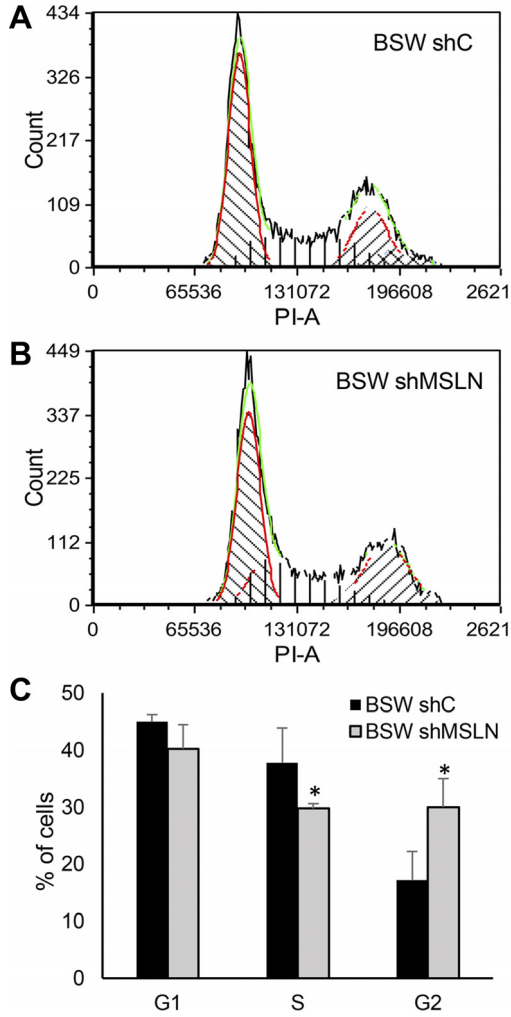

Fig. 7. Cell cycle progression is affected by MSLN. *A* and *B*: representative flow cytometry plot for propidium iodide stained BSW shC and BSW shMSLN cells. *C*: graphic representation of cell cycle distribution, determined from flow cytometry. FACS Express 5 software was used for analysis and proliferation statistics (green and red traces). $*P < 0.05$ vs. BSW shC.

Predictions as to the molecular mechanisms underlying MSLN-driven changes in BSW cell behavior were investigated by using IPA. These predictions were based on increased MSLN in BSW cells and fit well with our experimental observations as well as previously reported effects of MSLN in other cancer cell lines. Many of the predictions correlated with the observed aggressive behaviors, such as increases in MMP-9, which would contribute to the increased invasiveness of our SWCNT-transformed BSW cells. MSLN-induced increases in MMP have previously been linked to increased invasiveness in ovarian cancer cells (6).

One notable relationship is that TNF appears to induce MSLN, which in turn increases IL-6. IL-6 is known to stimulate TNF, creating a potential positive feedback loop that could markedly increase both MSLN and IL-6. IL-6 is an inflammatory chemokine that may serve as an important intermediate between MSLN overexpression and MSLN-induced aggressive behaviors. Specifically, IL-6 promotes cell growth, chemoresistance, anchorage-independent cell growth, and invasiveness (4, 17) and is overexpressed in MSLN-expressing pancreatic cancer cells (4, 41). It appears likely that MSLN does not directly induce IL-6; rather, MSLN activates NF-kB, which in turn induces IL-6 production (3).

Additionally, higher levels of MSLN tend to correlate with signs of inflammatory responses, including the induction of IL-6 (3), degradation of extracellular matrix by matrix metalloproteinases (6), and changes in attachment mediators (15, 50). Our IPA analysis also suggests that MSLN induces TNF-a, a key proinflammatory cytokine with an important role in lung cancer development. Typically an immune or inflammatory response to tissue damage or foreign particles will resolve as the particles clear and the environment returns to normal. The biopersistence of CNTs, however, would trigger a continuous inflammatory response, which can form a positive feedback loop to further increase MSLN expression. The similar biopersistence of CNTs and asbestos could also explain why MSLN is increased in nearly all mesotheliomas.

Increases in MSLN expression were also predicted by IPA to increase cyclin E, a cell cycle regulator that promotes the G1/S phase transition and is frequently dysregulated in cancer cells (14). We demonstrated that MSLN induced cyclin E in BSW cells. Elevated cyclin E has been found in pancreatic cells transformed to overexpress MSLN, where it was suggested that MSLN induces cyclin E through an IL-6/Stat3 pathway (3). This is a plausible mechanism for the increase in cyclin E in the BSW cells as well, particularly considering that IPA predicted MSLN-induced increases in both IL-6 and cyclin E.

In addition to verifying that MSLN knockdown did exhibit decreased cyclin E expression, we found that knockdown of MSLN shifted the proportion of cells in G2 and S phase of the cell cycle. After MSLN and, by extension, cyclin E knockdown, the expected decrease in S phase population was coupled with an increase in the G2 population. MSLN knockdown in mesothelioma cells also resulted in a decrease of the S phase population (24). IPA suggests that decreased cyclins A and B expression coupled with inhibited CDK1, which promotes G1/S and G2/M transition, found in the BSW line independent of MSLN expression, potentially contributed to increases in G2 population. The increased cyclin E in the MSLN-overexpressing cells may overcome the inhibitory effects of decreased cyclins A and B. This effect would be reversed when MSLN, and consequently cyclin E, expression is reduced.

As cyclin E drives cell cycle progression via G1/S transition, increased cyclin E is expected to increase cell proliferation. We found that, while BSW cells proliferate three times faster than BEAS-2B cells, knocking down MSLN in the BSW cells reduced their proliferation rate 2.5 times, nearly to the rate of the BEAS-2B cells. Similarly, H1299 lung cancer cells transduced to express MSLN proliferated 1.6 times faster than controls (16). MSLN overexpression has also been shown to increase the proliferation rate of pancreatic cancer cells (3, 24).

While we focused primarily on the contribution of cyclin E to the cell cycle dysregulation seen in BSW cells, our IPA results suggest that MSLN overexpression can affect additional cell proliferation and survival regulatory mechanisms. Specifically, MSLN may inhibit both p53 and the proapoptotic mediator BAX. Dysregulation of p53, a critical cell cycle regulator, is common in cancers. Typically p53 regulates G1/S cell cycle checkpoint, halting entry into the cell cycle when genetic damage is present (46). Inhibition of p53, such as that induced by MSLN, would allow cell proliferation regardless of genetic integrity. We have previously found that p53 is dysregulated in BSW cells (21, 47). The combined loss of p53-mediated damage control and cyclin E-driven increases in proliferation is amenable to the rapid accumulation of further mutations, which could manifest in vivo as more aggressive or treatment-resistant disease.

Additionally, inhibition of proapoptotic mediators, such as BAX, shifts the cell toward an antiapoptotic state. Although our analysis did not indicate changes in apoptotic regulators other than BAX, studies in pancreatic cancer cells suggest that MSLN overexpression leads to the decreases in both BAX and Bad (also proapoptotic), as well as increases in the antiapoptotic mediators Bcl-2 and Mcl-1 (41). BSW cells also exhibit apoptotic resistance, particularly in response to extrinsic mediators of apoptosis with BAX playing a potentially important signaling role (30).

Overall, we found that knocking down MSLN in the BSW cells reduced the severity of the malignant behaviors tested but did not completely eliminate them. This suggests that MSLN is important in the formation of both primary tumors and metastases, but is not the sole mechanism behind their formation. Even though MSLN may not be the primary driver of cancerous transformation, it appears to be heavily involved in a number of processes contributing to the final malignant phenotype and may make an attractive target for cancer therapeutics.

GRANTS

Support for this study was provided by National Institutes of Health Grants R01-ES-022968 and R01-EB-018857, National Science Foundation Grant CBET-1434503, and the WVU Cancer Institute (Sara C. Allen and James F. Allen Comp Lung Cancer Research Fund). Flow cytometric analysis was performed in the West Virginia University Flow Cytometry Core Facility, which is supported in part by National Institute of General Medical Sciences Grant P30-GM-103488. Imaging experiments and image analysis were performed in the West Virginia University Microscope Imaging Facility, which is supported by the West Virginia University Cancer Institute and National Center for Research Resources Grants P20-RR-016440, P30-RR-032138/GM103488, and P20-RR-016477.

DISCLOSURES

No conflicts of interest, financial or otherwise are declared by the author(s).

AUTHOR CONTRIBUTIONS

X.H., T.A.S., and Y.R. conception and design of research; X.H., E.D., T.A.S., C.Z.D., and L.W. performed experiments; X.H., E.D., T.A.S., and A.C. analyzed data; X.H., E.D., T.A.S., V.C., and Y.R. interpreted results of experiments; X.H., E.D., and T.A.S. prepared figures; X.H., E.D., T.A.S., V.C., and Y.R. edited and revised manuscript; E.D. drafted manuscript; Y.R. approved final version of manuscript.

REFERENCES

1. **Alvarez H, Rojas PL, Yong KT, Ding H, Xu G, Prasad PN, Wang J, Canto M, Eshleman JR, Montgomery EA, Maitra A.** Mesothelin is a specific biomarker of invasive cancer in the Barrett-associated adenocarcinoma progression model: translational implications for diagnosis and therapy. *Nanomedicine* 4: 295–301, 2008.
2. **Beck B, Blanpain C.** Unravelling cancer stem cell potential. *Nat Rev Cancer* 13: 727–738, 2013.
3. **Bharadwaj U, Li M, Chen C, Yao Q.** Mesothelin-induced pancreatic cancer cell proliferation involves alteration of cyclin E via activation of signal transducer and activator of transcription protein 3. *Mol Cancer Res* 6: 1755–1765, 2008.
4. **Bharadwaj U, Marin-Muller C, Li M, Chen C, Yao Q.** Mesothelin overexpression promotes autocrine IL-6/sIL-6R trans-signaling to stimulate pancreatic cancer cell proliferation. *Carcinogenesis* 32: 1013–1024, 2011.
5. **Borowicz S, Van Scoyk M, Avasarala S, Karuppusamy Rathinam MK, Tauler J, Bikkavilli RK, Winn RA.** The soft agar colony formation assay. *J Vis Exp* 27: e51998, 2014.
6. **Chang MC, Chen CA, Chen PJ, Chiang YC, Chen YL, Mao TL, Lin HW, Lin Chiang WH, Cheng WF.** Mesothelin enhances invasion of ovarian cancer by inducing MMP-7 through MAPK/ERK and JNK pathways. *Biochem J* 442: 293–302, 2012.
7. **Chen D, Stueckle TA, Luanpitpong S, Rojanasakul Y, Lu Y, Wang L.** Gene expression profile of human lung epithelial cells chronically exposed to single-walled carbon nanotubes. *Nanoscale Res Lett* 10, 2015.
8. **Drapkin R, Crum CP, Hecht JL.** Expression of candidate tumor markers in ovarian carcinoma and benign ovary: evidence for a link between epithelial phenotype and neoplasia. *Hum Pathol* 35: 1014–1021, 2004.
9. **Erdogan E, Demirkazik FB, Gulsun M, Ariyurek M, Emri S, Sak SD.** Incidental localized (solitary) mediastinal malignant mesothelioma. *Br J Radiol* 78: 858–861, 2005.
10. **Fisher C, Rider AE, Jun Han Z, Kumar S, Levchenko I, Ostrikov K.** Applications and nanotoxicity of carbon nanotubes and graphene in biomedicine. *J Nanomater* 2012: 315185, 2012.
11. **Gangwal AS, Brown JS, Wang A, Houck KA, Dix DJ, Kavlock RJ, Hubal EAC.** Informing selection of nanomaterial concentrations for ToxCast in vitro testing based on occupational exposure potential. *Environ Health Perspect* 119: 1539–1546.
12. **Hassan R, Remaley AT, Sampson ML, Zhang J, Cox DD, Pingpank J, Alexander R, Willingham M, Pastan I, Onda M.** Detection and quantitation of serum mesothelin, a tumor marker for patients with mesothelioma and ovarian cancer. *Clin Cancer Res* 12: 447–453, 2006.
13. **Ho M, Bera TK, Willingham MC, Onda M, Hassan R, FitzGerald D, Pastan I.** Mesothelin expression in human lung cancer. *Clin Cancer Res* 13: 1571–1575, 2007.
14. **Hwang HC, Clurman BE.** Cyclin E in normal and neoplastic cell cycles. *Oncogene* 24: 2776–2786, 2005.
15. **Ito T, Kajino K, Abe M, Sato K, Maekawa H, Sakurada M, Orita H, Wada R, Kajiyama Y, Hino O.** ERC/mesothelin is expressed in human gastric cancer tissues and cell lines. *Oncol Rep* 31: 27–33, 2014.
16. **Kachala SS, Bograd AJ, Villena-Vargas J, Suzuki K, Servais EL, Kadota K, Chou J, Sima CS, Vertes E, Rusch VW, Travis WD, Sadelain M, Adusumilli PS.** Mesothelin overexpression is a marker of tumor aggressiveness and is associated with reduced recurrence-free and overall survival in early-stage lung adenocarcinoma. *Clin Cancer Res* 20: 1020–1028, 2014.
17. **Kipps E, Tan DSP, Kaye SB.** Meeting the challenge of ascites in ovarian cancer: new avenues for therapy and research. *Nat Rev Cancer* 13: 273–282, 2013.
18. **Kramer N, Walzl A, Unger C, Rosner M, Krupitza G, Hengstschläger M, Dolznig H.** In vitro cell migration and invasion assays. *Mutat Res* 752: 10–24, 2013.
19. **Li M, Bharadwaj U, Zhang R, Zhang S, Mu H, Fisher WE, Brunicardi FC, Chen C, Yao Q.** Mesothelin is a malignant factor and therapeutic vaccine target for pancreatic cancer. *Mol Cancer Ther* 7: 286–296, 2008.
20. **Lohcharoenkal W, Wang L, Stueckle TA, Dinu CZ, Castranova V, Liu Y, Rojanasakul Y.** Chronic exposure to carbon nanotubes induces invasion of human mesothelial cells through matrix metalloproteinase-2. *ACS Nano* 7: 7711–7723, 2013.
21. **Luanpitpong S, Wang L, Castranova V, Rojanasakul Y.** Induction of stem-like cells with malignant properties by chronic exposure of human lung epithelial cells to single-walled carbon nanotubes. *Part Fibre Toxicol* 11: 22–40, 2014.
22. **Luanpitpong S, Wang L, Davidson DC, Riedel H, Rojanasakul Y.** Carcinogenic Potential for High Aspect Ratio Carbon Nanomaterials. *Environ Sci Nano* 3: 483–493, 2016.
23. **Luanpitpong S, Wang L, Stueckle TA, Tse W, Chen YC, Rojanasakul Y.** Caveolin-1 regulates lung cancer stem-like cell induction and p53 inactivation in carbon nanotube-driven tumorigenesis. *Oncotarget* 5: 3541–3554, 2014.
24. **Melaiu O, Stebbing J, Lombardo Y, Bracci E, Uehara N, Bonotti A, Cristaudo A, Foddis R, Mutti L, Barale R, Gemignani F, Giamas G, Landi S.** MSLN gene silencing has an anti-malignant effect on cell lines overexpressing mesothelin deriving from malignant pleural mesothelioma. *PLoS One* 9: e85935, 2014.
25. **Miettinen M, Sarlomo-rikala M.** Expression of calretinin, thrombomodulin, keratin 5, and mesothelin in lung carcinomas of different types an immunohistochemical analysis of 596 tumors in comparison with epithelioid mesotheliomas of the pleura. *Am J Surg Pathol* 27: 150–158, 2003.
26. **Ordóñez NG.** The immunohistochemical diagnosis of mesothelioma a comparative study of epithelioid mesothelioma and lung adenocarcinoma. *Am J Surg Pathol* 27: 1031–1051, 2003.
27. **Ordóñez NG.** Application of mesothelin immunostaining in tumor diagnosis. *Am J Surg Pathol* 27: 1418–1428, 2003.
28. **Park YH, Kim D, Dai J, Zhang Z.** Human bronchial epithelial BEAS-2B cells, an appropriate in vitro model to study heavy metals induced carcinogenesis. *Toxicol Appl Pharmacol* 287: 240–245, 2015.
29. **Pastan I, Hassan R.** Discovery of mesothelin and exploiting it as a target for immunotherapy. *Cancer Res* 74: 2907–2912, 2014.
30. **Pongrakhananon V, Luanpitpong S, Stueckle TA, Wang L, Nimmannit U, Rojanasakul Y.** Carbon nanotubes induce apoptosis resistance of human lung epithelial cells through FLICE-inhibitory protein. *Toxicol Sci* 143: 499–511, 2015.
31. **Rump A, Morikawa Y, Tanaka M, Minami S, Umesaki N, Takeuchi M, Miyajima A.** Binding of ovarian cancer antigen CA125/MUC16 to mesothelin mediates cell adhesion. *J Biol Chem* 279: 9190–9198, 2004.
32. **Sargent LM, Porter DW, Staska LM, Hubbs AF, Lowry DT, Battelli L, Siegrist KJ, Kashon ML, Mercer RR, Bauer AK, Chen BT, Salisbury JL, Frazer D, McKinney W, Andrew M, Tsuruoka S, Endo M, Fluharty KL, Castranova V, Reynolds SH.** Promotion of lung adenocarcinoma following inhalation exposure to multi-walled carbon nanotubes. *Part Fibre Toxicol* 11: 3, 2014.
33. **Shimizu A, Hirono S, Tani M, Kawai M, Okada KI, Miyazawa M, Kitahata Y, Nakamura Y, Noda T, Yokoyama S, Yamaue H.** Coexpression of MUC16 and mesothelin is related to the invasion process in pancreatic ductal adenocarcinoma. *Cancer Sci* 103: 739–746, 2012.
34. **Shvedova AA, Yanamala N, Kisin ER, Tkach AV, Murray AR, Hubbs A, Chirila MM, Keohavong P, Sycheva LP, Kagan VE, Castranova V.** Long-term effects of carbon containing engineered nanomaterials and asbestos in the lung: one year postexposure comparisons. *Am J Physiol Lung Cell Mol Physiol* 306: L170–L182, 2014.
35. **Shvedova AA, Kisin E, Murray AR, Johnson VJ, Gorelik O, Arepalli S, Hubbs AF, Mercer RR, Keohavong P, Sussman N, Jin J, Yin J, Stone S, Chen BT, Deye G, Maynard A, Castranova V, Baron PA, Kagan VE.** Inhalation vs. aspiration of single-walled carbon nanotubes in C57BL/6 mice: inflammation, fibrosis, oxidative stress, and mutagenesis. *Am J Physiol Lung Cell Mol Physiol* 295: L552–L565, 2008.
36. **Siegrist KJ, Reynolds SH, Kashon ML, Lowry DT, Dong C, Hubbs AF, Young SH, Salisbury JL, Porter DW, Benkovic a S, McCawley M, Keane MJ, Mastovich JT, Bunker KL, Cena LG, Sparrow MC, Sturgeon JL, Dinu CZ, Sargent LM.** Genotoxicity of multi-walled carbon nanotubes at occupationally relevant doses. *Part Fibre Toxicol* 11: 6, 2014.
37. **Smolková P, Nakládalová M, Zapletalová J, Jakubec P, Vildová H, Kolek V, Petřek M, Nakládal Z.** Validity of mesothelin in occupational medicine practice. *Int J Occup Med Environ Health* 29: 395–404, 2016.
38. **Stella GM.** Carbon nanotubes and pleural damage: perspectives of nanosafety in the light of asbestos experience. *Biointerphases* 6: P1–17, 2011.
39. **Stueckle TA, Lu Y, Davis ME, Wang L, Jiang BH, Holaskova I, Schafer R, Barnett JB, Rojanasakul Y.** Chronic occupational exposure

to arsenic induces carcinogenic gene signaling networks and neoplastic transformation in human lung epithelial cells. *Toxicol Appl Pharmacol* 261: 204–216, 2012.

40. **Sun H, Clancy HA, Kluz T, Zavadil J, Costa M.** Comparison of gene expression profiles in chromate transformed BEAS-2B cells. *PLoS One* 6: e17982, 2011.
41. **Tang Z, Qian M, Ho M.** The role of mesothelin in tumor progression and targeted therapy. *Anticancer Agents Med Chem* 13: 276–280, 2013.
42. **Thurnherr T, Brandenberger C, Fischer K, Diener L, Manser P, Maeder-Althaus X, Kaiser JP, Krug HF, Rothen-Rutishauser B, Wick P.** A comparison of acute and long-term effects of industrial multiwalled carbon nanotubes on human lung and immune cells in vitro. *Toxicol Lett* 200: 176–186, 2011.
43. **Uehara N, Matsuoka Y, Tsubura A.** Mesothelin promotes anchorage-independent growth and prevents anoikis via extracellular signal-regulated kinase signaling pathway in human breast cancer cells. *Mol Cancer Res* 6: 186–193, 2008.
44. **Vales G, Rubio L, Marcos R.** Genotoxic and cell-transformation effects of multi-walled carbon nanotubes (MWCNT) following in vitro sub-chronic exposures. *J Hazard Mater* 306: 193–202, 2015.
45. **Veljkovic E, Jiricny J, Menigatti M, Rehrauer H, Han W.** Chronic exposure to cigarette smoke condensate in vitro induces epithelial to mesenchymal transition-like changes in human bronchial epithelial cells, BEAS-2B. *Toxicol Vitr* 25: 446–453, 2011.
46. **Vermeulen K, Van Bockstaele DR, Berneman ZN.** The cell cycle: a review of regulation, deregulation and therapeutic targets in cancer. *Cell Prolif* 36: 131–149, 2003.
47. **Wang L, Luanpitpong S, Castranova V, Tse W, Lu Y, Pongrakhananon V, Rojanasakul Y.** Carbon nanotubes induce malignant transformation and tumorigenesis of human lung epithelial cells. *Nano Lett* 11: 2796–2803, 2011.
48. **Wang L, Stueckle TA, Mishra A, Derk R, Meighan T, Castranova V, Rojanasakul Y.** Neoplastic-like transformation effect of single-walled and multi-walled carbon nanotubes compared with asbestos on human lung small airway epithelial cells. *Nanotoxicology* 8: 485–507, 2014.
49. **Wang Y, Yu Y, Tsuyada a Ren X, Wu X, Stubblefield K, Rankin-Gee EK, Wang SE.** Transforming growth factor-β regulates the sphere-initiating stem cell-like feature in breast cancer through miRNA-181 and ATM. *Oncogene* 30: 1470–1480, 2011.
50. **Zhang D, Kobayashi T, Kojima T, Kanenishi K, Hagiwara Y, Abe M, Okura H, Hamano Y, Sun G, Maeda M, Jishage K, Noda T, Hino O.** Deficiency of the Erc/mesothelin gene ameliorates renal carcinogenesis in Tsc2 knockout mice. *Cancer Sci* 102: 720–727, 2011.